Dual Solutions in Mixed Convection Boundary Layer Flow: A Stability Analysis

Anuar Ishak

Abstract—The mixed convection stagnation point flow toward a vertical plate is investigated. The external flow impinges normal to the heated plate and the surface temperature is assumed to vary linearly with the distance from the stagnation point. The governing partial differential equations are transformed into a set of ordinary differential equations, which are then solved numerically using MATLAB routine boundary value problem solver bvp4c. Numerical results show that dual solutions are possible for a certain range of the mixed convection parameter. A stability analysis is performed to determine which solution is linearly stable and physically realizable.

Keywords—Dual solutions, heat transfer, mixed convection, stability analysis.

I. INTRODUCTION

THE problem of stagnation point flow over a flat plate was considered by Hiemenz (see [1]) who discovered that this flow can be analyzed exactly by the Navier-Stokes equations. The temperature distribution of this flow was analyzed by Goldstein [2]. This problem was then extended to the axisymmetric flow by Homann (see [1]) for the velocity field and by Sibulkin [3] for the temperature field.

The mixed convection stagnation point flow toward a vertical plate was considered by Ramachandran et al. [4] where the existence of dual solutions for the opposing flow case was reported. Ishak et al. [5] then considered the flow toward a permeable surface and reported that the second solutions obtained by Ramachandran et al. [4] continue further to the assisting flow regime.

The objective of the present paper is to investigate the stability of the solutions reported previously by Ramachandran et al. [4] and Ishak et al. [5].

II. MATHEMATICAL FORMULATION

Consider a steady stagnation point flow of a viscous fluid toward a vertical plate as shown in Fig. 1. The external flow impinges normal to the plate, $u_e(x)$, and the surface temperature, $T_w(x)$, are assumed to vary linearly with the distance from the stagnation point, i.e. $u_e(x) = ax$ and $T_w(x) = T_\infty + bx$, where a and b are constants and T_∞ is the ambient temperature. Under these assumptions, the steady governing continuity, momentum and energy boundary layer equations are [4], [5]

A. Ishak is with the School of Mathematical Sciences, Faculty of Science and Technology, Universiti Kebangsaan Malaysia, 43600 UKM Bangi, Malaysia (phone: +603-8921-5785; fax: +603-8925-4519; e-mail: anuarishak@yahoo.com).

$$\frac{\partial u}{\partial x} + \frac{\partial v}{\partial y} = 0 \tag{1}$$

$$u\frac{\partial u}{\partial x} + v\frac{\partial u}{\partial y} = u_e \frac{du_e}{dx} + v\frac{\partial^2 u}{\partial y^2} + g\beta(T - T_{\infty})$$
 (2)

$$u\frac{\partial T}{\partial x} + v\frac{\partial T}{\partial y} = \alpha \frac{\partial^2 T}{\partial y^2}$$
 (3)

where u and v are the velocity components along the x- and y-axis respectively, T is the fluid temperature, α is the thermal diffusivity, β is the thermal expansion coefficient, v is the kinematic viscosity and g is the acceleration due to gravity.

The equations (1)-(3) are subjected to the boundary conditions

$$u = 0, \quad v = 0, \quad T = T_w \quad \text{at} \quad y = 0,$$

 $u \to u_s(x), \quad T \to T_w \quad \text{as} \quad y \to \infty.$ (4)

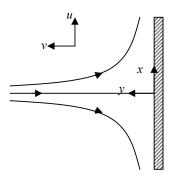


Fig. 1 Physical model and coordinate system

In order to solve (1) to (3) subject to the boundary conditions (4), we introduce the following similarity transformation:

$$\eta = \left(\frac{u_e}{vx}\right)^{1/2} y, \quad \psi = \left(vxu_e\right)^{1/2} f(\eta), \quad \theta(\eta) = \frac{T - T_{\infty}}{T_w - T_{\infty}}, \quad (5)$$

where ψ is the stream function defined as $u = \partial \psi / \partial y$ and $v = -\partial \psi / \partial x$, which identically satisfies (1).

Substituting (5) into (2) and (3) we obtain the following ordinary differential (similarity) equations

$$f''' + ff'' + 1 - f'^{2} + \lambda \theta = 0$$
 (6)

$$\frac{1}{\Pr}\theta'' + f\theta' - f'\theta = 0 \tag{7}$$

where prime denotes differentiation with respect to η , $\lambda = g\beta b/a^2$ is the buoyancy or mixed convection parameter and $\Pr = v/\alpha$ is the Prandtl number. The boundary conditions (4) become

$$f(0) = 0, \quad f'(0) = 0, \quad \theta(0) = 1$$

 $f'(\eta) \to 1, \quad \theta(\eta) \to 0 \quad \text{as} \quad \eta \to \infty.$ (8)

The quantities of physical interest are the skin friction coefficient C_f , and the local Nusselt number Nu_x , which are defined as

$$C_f = \frac{\tau_w}{\rho u_e^2(x)}, \ Nu_x = \frac{x \, q_w}{k \, (T_w - T_\infty)}$$
 (9)

where τ_w is the surface shear stress along the plate and q_w is the heat flux from the plate, which are defined as

$$\tau_{w} = \mu \left(\frac{\partial u}{\partial y} \right)_{v=0}, \quad q_{w} = -k \left(\frac{\partial T}{\partial y} \right)_{v=0}$$
(10)

Using (5) we get

$$\operatorname{Re}_{x}^{1/2} C_{f} = f''(0), \operatorname{Re}_{x}^{-1/2} Nu_{x} = -\theta'(0)$$
 (11)

where $Re_x = u_a x / v$ is the local Reynolds number.

III. STABILITY OF SOLUTIONS

In order to perform a stability analysis, we consider the unsteady problem. Equation (1) holds, while (2) and (3) are replaced by

$$\frac{\partial u}{\partial t} + u \frac{\partial u}{\partial x} + v \frac{\partial u}{\partial y} = \frac{\partial u_e}{\partial t} + u_e \frac{du_e}{dt} + v \frac{\partial^2 u}{\partial y^2} + g \beta (T - T_\infty)$$
(12)

$$\frac{\partial T}{\partial t} + u \frac{\partial T}{\partial x} + v \frac{\partial T}{\partial y} = \alpha \frac{\partial^2 T}{\partial y^2}$$
 (13)

where t denotes the time. Based on the variables (5), we introduce the following new dimensionless variables:

$$\eta = \left(\frac{u_e}{vx}\right)^{1/2} y, \quad \psi = \left(vxu_e\right)^{1/2} f(\eta, \tau), \\
\theta(\eta, \tau) = \frac{T - T_{\infty}}{T - T}, \qquad \tau = at$$
(14)

so that (2) and (3) can be written as

$$\frac{\partial^3 f}{\partial \eta^3} + f \frac{\partial^2 f}{\partial \eta^2} - \left(\frac{\partial f}{\partial \eta} \right)^2 + 1 - \frac{\partial^2 f}{\partial \eta \partial \tau} + \lambda \theta = 0$$
 (15)

$$\frac{1}{\text{Pr}}\frac{\partial^2 \theta}{\partial \eta^2} + f \frac{\partial \theta}{\partial \eta} - \theta \frac{\partial f}{\partial \eta} - \frac{\partial \theta}{\partial \tau} = 0$$
 (16)

and are subjected to the boundary conditions

$$f(0,\tau) = 0$$
, $\frac{\partial f}{\partial \eta}(0,\tau) = 0$, $\theta(0,\tau) = 1$
 $\frac{\partial f}{\partial \eta}(\eta,\tau) \to 1$, $\theta(\eta,\tau) \to 0$ as $\eta \to \infty$

To test the stability of the steady flow solution $f(\eta) = f_0(\eta)$ and $\theta(\eta) = \theta_0(\eta)$ satisfying the boundary-value problem (1)-(4), we write (see [6]-[8]),

$$f(\eta, \tau) = f_0(\eta) + e^{-\gamma \tau} F(\eta, \tau),$$

$$\theta(\eta, \tau) = \theta_0(\eta) + e^{-\gamma \tau} G(\eta, \tau),$$
(18)

where γ is an unknown eigenvalue, and $F(\eta,\tau)$ and $G(\eta,\tau)$ are small relative to $f_0(\eta)$ and $\theta_0(\eta)$. Solutions of the eigenvalue problem (15)-(17) give an infinite set of eigenvalues $\gamma_1 < \gamma_2 < \cdots$; if the smallest eigenvalue is negative, there is an initial growth of disturbances and the flow is unstable; but when γ_1 is positive, there is an initial decay and the flow is stable. Introducing (18) into (15) and (16), we get the following linearized problem

$$\frac{\partial^{3} F}{\partial \eta^{3}} + f_{0} \frac{\partial^{2} F}{\partial \eta^{2}} + f_{0}'' F - \left(2f_{0}' - \gamma\right) \frac{\partial F}{\partial \eta} - \frac{\partial^{2} F}{\partial \eta \partial \tau} + \lambda G = 0 \qquad (19)$$

$$\frac{1}{\Pr} \frac{\partial^2 G}{\partial n^2} + f_0 \frac{\partial G}{\partial n} + \theta_0' F + \gamma G - f_0' G - \theta_0 \frac{\partial F}{\partial n} - \frac{\partial G}{\partial \tau} = 0 \quad (20)$$

along with the boundary conditions

$$F(0,\tau) = 0, \quad \frac{\partial F}{\partial \eta}(0,\tau) = 0, \quad G(0,\tau) = 0,$$

$$\frac{\partial F}{\partial \eta}(\eta,\tau) \to 0, \quad G(\eta,\tau) \to 0 \quad \text{as} \quad \eta \to \infty$$
(21)

The solutions $f(\eta)=f_0(\eta)$ and $\theta(\eta)=\theta_0(\eta)$ of the steady equations (6) and (7) are obtained by setting $\tau=0$. Hence $F=F_0(\eta)$ and $G=G_0(\eta)$ in (19) and (20) identify initial growth or decay of the solution (18). In this respect, we have to solve the linear eigenvalue problem

$$F_0''' + f_0 F_0'' + f_0'' F_0 - (2f_0' - \gamma) F_0' + \lambda G_0 = 0$$
 (22)

$$\frac{1}{\Pr}G_0'' + f_0G_0' + F_0\theta_0' + \gamma G_0 - G_0f_0' - F_0'\theta_0 = 0$$
 (23)

along with the boundary conditions

$$F_0(0) = 0, \quad F_0'(0) = 0, \quad G_0(0) = 0$$
 (24)
 $F_0'(\eta) \to 0, \quad G_0(\eta) \to 0 \quad \text{as} \quad \eta \to \infty$

It should be stated that for particular values of Pr and γ , the stability of the corresponding steady flow solutions $f_0(\eta)$ and $\theta_0(\eta)$ are determined by the smallest eigenvalue γ . As it has been suggested by Harris et al. [9], the range of possible eigenvalues can be determined by relaxing a boundary condition on $F_0(\eta)$ or $G_0(\eta)$. For the present problem, we relax the condition that $F_0'(\eta) \to 0$ as $\eta \to \infty$ and for a fixed value of γ we solve the system (26, 27, 28) along with the new boundary condition $F_0''(0) = 1$.

IV. RESULTS AND DISCUSSION

The system of equations (6)-(8) was solved numerically using the bvp4c solver in MATLAB software. In order to validate the numerical results obtained, we have compared our results with those reported by Ramachandran et al. [4], Ishak et al. [5], Hassanien and Gorla [10], Devi et al. [11] and Lok et al. [12], [13], which showed an excellent agreement. However, due to space constraint, only the results reported in [4] are presented in Tables I and II.

TABLE I VALUES OF f''(0) FOR DIFFERENT VALUES OF Pr

Pr	Ramachandran et al. [4]	Present results	
		First solution	Second solution
0.7	1.7063	1.7063	1.2387
1	-	1.6754	1.1332
7	1.5179	1.5179	0.5824
10	-	1.4928	0.4958
20	1.4485	1.4485	0.3436

TABLE II VALUES OF - heta'(0) FOR DIFFERENT VALUES OF PI

Pr	Ramachandran et _ al. [4]	Present results	
		First solution	Second solution
0.7	0.7641	0.7641	1.0226
1	-	0.8708	1.1691
7	1.7224	1.7224	2.2192
10	-	1.9446	2.4940
20	2.4576	2.4576	3.1646

The variations of the skin friction coefficient f''(0) and the local Nusselt number $-\theta'(0)$ are presented in Figs. 2 and 3, respectively. Different from the results by Ramachandran et al. [4], who reported the existence of dual solutions only for the buoyancy opposing flow case ($\lambda < 0$), these figures show the existence of dual solutions for both buoyancy assisting ($\lambda > 0$) and opposing ($\lambda < 0$) flows. Both solutions exist up to a critical value of λ , i.e. $\lambda = \lambda_c$, beyond which no solution exist. The validity of dual solutions presented in Figs. 2 and 3 is supported by the velocity and temperature profiles presented

in Figs. 4 and 5, respectively. It is seen in these figures that there are two different profiles for the same value of parameter λ , where both satisfy the far field boundary conditions asymptotically.

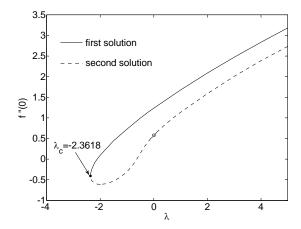


Fig. 2 Variation of the skin friction coefficient f''(0) with λ when Pr = 1

To test the stability of the solutions, we perform a stability analysis and find the eigenvalues γ in (18). If the smallest eigenvalue is negative, there is an initial growth of disturbances and the flow is unstable; while when the smallest eigenvalue is positive, there is an initial decay and the flow is stable. The smallest eigenvalues γ for selected values of λ are presented in Table III which shows that γ is positive for the first solution and negative for the second solution. Thus, the first solution is stable, while the second solution is unstable. The transition from positive (stable) to negative (unstable) values of γ occurs at the turning points of the parametric solution curves ($\lambda = \lambda_e$), which is shown in Figs. 2 and 3.

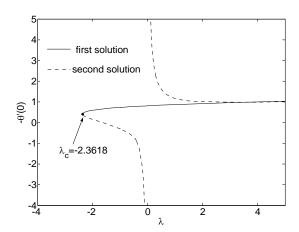


Fig. 3 Variation of the local Nusselt number $-\theta'(0)$ with λ when Pr = 1

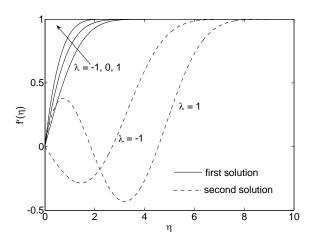


Fig. 4 Velocity profiles for different values of λ when Pr = 1

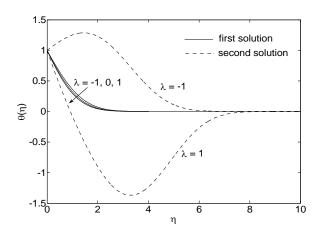


Fig. 5 Temperature profiles for different values of λ when Pr = 1

TABLE III Smallest Eigen values γ at Several Values of $\,\lambda$

First solution	Second solution
0	0
0.7912	-0.7091
1.6523	-1.2052
3.0627	-
4.6768	-1.6875
5.1398	-1.7980
5.5331	-1.8811
	0 0.7912 1.6523 3.0627 4.6768 5.1398

Although the second solution is unstable and deprive of physical significant, it is still of mathematical interest since the solution is also a solution to the system of differential equations. The second solution may have more realistic meaning in other situations. For the first solution which is linearly stable and likely physically realizable, the skin friction coefficient increases as λ increases, see Fig. 2, which in turn increase the local Nusselt number (represents the heat transfer rate at the surface) as presented in Fig. 3.

V.CONCLUSIONS

Numerical results showed that dual solutions are possible for a certain range of the mixed convection parameter. The first and the second solutions meet at the critical point of the mixed convection parameter, beyond which no solution exists. The stability analysis showed that there is an initial decay for the first solution, while there is an initial growth of disturbances for the second solution. Thus, the first solution is linearly stable, while the second solution is linearly unstable. Both the skin friction coefficient and the heat transfer rate at the surface increase as the buoyancy force increases.

ACKNOWLEDGMENT

The financial support received from the Universiti Kebangsaan Malaysia (Project Code: DIP-2012-31) is gratefully acknowledged.

REFERENCES

- [1] F.M. White, Viscous Fluid Flow. Boston: McGraw Hill, 2006.
- [2] S. Goldstein, Modern Developments in Fluid Dynamics. London: Oxford University Press, 1938.
- [3] M. Sibulkin, "Heat transfer near the forward stagnation point of a body of revolution," J. Aeronaut. Sci. 19 (1952) 570-571.
- [4] N. Ramachandran, T.S. Chen, B.F. Armaly, Mixed convection in stagnation flows adjacent to a vertical surfaces, ASME J. Heat Transfer 110 (1988) 373–377.
- [5] A. Ishak, R. Nazar, I. Pop, Dual solutions in mixed convection flow near a stagnation point on a vertical porous plate, *Int. J. Therm. Sci.*, 47 (2008) 417-422.
- [6] P.D. Weidman, D.G. Kubitschek and A.M.J. Davis, "The effect of transpiration on self-similar boundary layer flow over moving surfaces," *Int. J. Eng. Sci.*, vol. 44, pp. 730-737, 2006.
- [7] A. Postelnicu and I. Pop, "Falkner–Skan boundary layer flow of a power-law fluid past a stretching wedge," *Appl. Math. Comput.* vol. 217, pp. 4359-4368, 2011.
- [8] A.V. Rosca and I. Pop, "Flow and heat transfer over a vertical permeable stretching/ shrinking sheet with a second order slip," *Int. J. Heat Mass Transfer*, vol. 60, 355-364, 2013.
- [9] S.D. Harris, D.B. Ingham and I. Pop, "Mixed convection boundary-layer flow near the stagnation point on a vertical surface in a porous medium: Brinkman model with slip," *Transport Porous Media*, vol. 77, pp. 267-285, 2009.
- [10] I.A. Hassanien, R.S.R. Gorla, Combined forced and free convection in stagnation flows of micropolar fluids over vertical non-isothermal surfaces, Int. J. Engng. Sci. 28 (1990) 783–792.
- [11] C.D.S. Devi, H.S. Takhar, G. Nath, Unsteady mixed convection flow in stagnation region adjacent to a vertical surface, Heat Mass Transfer 26 (1991) 71–79.
- [12] Y.Y. Lok, N. Amin, D. Campean, I. Pop, Steady mixed convection flow of a micropolar fluid near the stagnation point on a vertical surface, Int. J. Numer. Methods Heat Fluid Flow 15 (2005) 654–670.
- [13] Y.Y. Lok, N. Amin, I. Pop, Unsteady mixed convection flow of a micropolar fluid near the stagnation point on a vertical surface, Int. J. Thermal Sci. 45 (2006) 1149–1157.